Receptor-Targeted Liposomal Delivery of Boron-Containing Cholesterol Mimics for Boron Neutron Capture Therapy (BNCT)

B.T.S. Thirumamagal,[†,‡] Xiaobin B. Zhao,[†,§] Achintya K. Bandyopadhyaya,[‡] Sureshbabu Narayanasamy,[‡] Jayaseharan Johnsamuel,[‡] Rohit Tiwari,[‡] Danold W. Golightly,[∥] Vimalkumar Patel,[○] Brian T. Jehning,[○] Marina V. Backer,[○] Rolf F. Barth,[⊥,#] Robert J. Lee,[§,#,▽] Joseph M. Backer,[○] and Werner Tjarks*[,‡,#]

Division of Medicinal Chemistry & Pharmacognosy, Division of Pharmaceutics, Department of Civil and Environmental Engineering, Department of Pathology, Comprehensive Cancer Center, and Nanoscale Science and Engineering Center of The Ohio State University, Columbus, Ohio 43210, and SibTech, Inc., Newington, Connecticut 06111. Received March 26, 2006; Revised Manuscript Received June 16, 2006

Liposomes have been a main focus of tumor-selective boron delivery strategies in boron neutron capture therapy (BNCT), a binary method for the treatment of cancer that is based on the nuclear reaction between boron atoms and low-energy thermal neutrons. Three novel carboranyl cholesterol derivatives were prepared as lipid bilayer components for the construction of nontargeted and receptor-targeted boronated liposomes for BNCT. A major structural feature of these novel boronated cholesterol mimics is the replacement of the B and the C ring of cholesterol with a carborane cluster. Computational analyses indicated that all three boronated compounds have structural features and physicochemical properties that are very similar to those of cholesterol. One of the synthesized boronated cholesterol mimics was stably incorporated into non-, folate receptor (FR)-, and vascular endothelial growth factor receptor-2 (VEGFR-2)-targeted liposomes. No major differences were found in appearance, size distribution, and lamellarity between conventional dipalmitoylphosphatidylcholine (DPPC)/cholesterol liposomes, nontargeted, and FR-targeted liposomal formulations of this carboranyl cholesterol derivative. FR-targeted boronated liposomes were taken up extensively in FR overexpressing KB cells in vitro, and the uptake was effectively blocked in the presence of free folate. In contrast, a boronated cholesterol mimic incorporated into nontargeted liposomes showed significantly lower cellular uptake. There was no apparent in vitro cytotoxicity in FR overexpressing KB cells and VEGFR-2 overexpressing 293/KDR cells when these were incubated with boronated FR- and (VEGFR-2)-targeted liposomes, respectively, although the former accumulated extensively in KB cells and the latter effectively interacted with VEGFR-2 by causing autophosphorylation and protecting 293/KDR cells from SLT (Shiga-like toxin)−VEGF cytotoxicity.

INTRODUCTION

Boron neutron capture therapy (BNCT) is a binary method for the treatment of cancer (*1*), which is based on the nuclear reaction between boron atoms and low-energy thermal neutrons. Naturally occurring elemental boron has two stable isotopes, namely, boron-10 (^{10}B) and boron-11 (^{11}B). The abundant isotope is ^{11}B (around 80%); however, the most distinguishing property of ^{10}B is its high neutron capture cross section for thermal (slow) neutrons. Hence, the reaction of a neutron with ^{10}B yields two charged particles, a ^{4}He nucleus and a ^{7}Li nucleus, each of which are able to kill tumor cells due to their high linear energy transfer. For successful BNCT, a minimum of 20−30 μg of nonradioactive ^{10}B per gram of tumor tissue is required. Another key requirement for the success of BNCT is the selective delivery of high amounts of boronated compounds to tumor cells, while at the same time, the boron concentration in the cells of surrounding normal tissue should be kept low to minimize the damage to normal tissue.

Liposomes have been a main focus of tumor selective boron delivery strategies in BNCT since research activities in this area were initiated by Hawthorne (*2*) and Yanagie (*3*) in the early 1990s. Design strategies for boron-containing liposomes for BNCT centered on both nontargeted (*4*, *5*), and tumor-targeted formulations. The latter included liposomes conjugated to transferrin (*6*), the epidermal growth factor (EGF) (*7*), antibodies (*8*), α (v)-integrin specific arginine−glycine−aspartate (RGD) peptides (*9*), and folic acid (*10*, *11*). Most liposomes designed for BNCT contained hydrophilic low molecular weight boron agents, which presumably localized in the aqueous core of the liposomes during preparation. These boron agents include sodium borocaptate (BSH) (*12*, *13*) and boronophenylalanine (BPA) (*14*), both of which have been used in clinical BNCT (*1*), negatively charged boron clusters with or without simple substitution patterns (*2*, *15*), as well as carborane cage-substituted polyamines (*11*), acridines (*7*, *8*), porphyrins (*16*), carbohydrates (*17*), and nucleosides (*18*).

Phospholipids are common lipid bilayer components of liposomes and have proven to be effective anchors for boron entities in the form of dual- (*19*, *20*) or single- (*10*, *21*) chain *nido*-carboranyl phospholipid mimics. Cholesterol is another major component of the mammalian cell membrane and most liposomal formulations. It is transported in the blood stream by low-density lipoprotein (LDL). Owing to its natural carrier capability and receptor-targeting specificity, LDL has been

* Corresponding author. Werner Tjarks, The Ohio State University, College of Pharmacy, 500 West 12th Avenue, Columbus, OH 43210; phone (614) 292 7624, fax (614) 292 2435, e-mail: tjarks.1@osu.edu.
† B.T.S.T. and X.B.Z made equal contributions to this manuscript.
‡ Division of Medicinal Chemistry & Pharmacognosy.
§ Division of Pharmaceutics.
∥ Department of Civil and Environmental Engineering.
⊥ Department of Pathology.
Comprehensive Cancer Center.
▽ Nanoscale Science and Engineering Center.
○ SibTech, Inc.

10.1021/bc060075d CCC: $33.50
Published on Web 08/15/2006

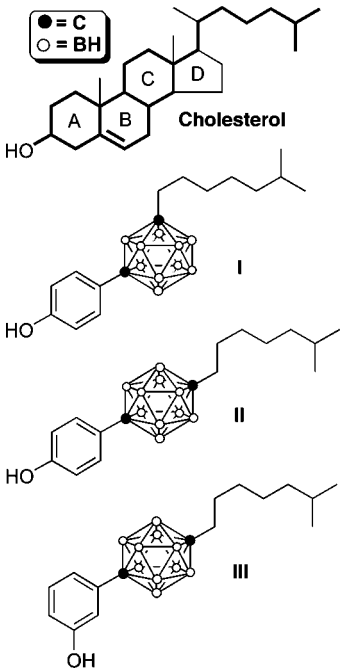

Figure 1. Structures of cholesterol and boronated cholesterol mimics **I**−**III.**

extensively studied as a drug carrier (*22*). Therefore, the development of boron-containing compounds that mimic physiological cholesterol and cholesterol esters is potentially an effective approach for boron delivery to cancer cells via both liposomes and LDL, and thus, extensive efforts in BNCT drug development have focused on such structures (*23*−*30*).

To the best of our knowledge, all synthetic approaches directed toward boron-containing cholesterol derivatives have focused on the attachment of carboranyl moieties to the hydroxyl group of cholesterol via ether or ester linkages. In the present manuscript, we report a novel strategy for the design and synthesis of carboranyl cholesterol mimics. This design strategy is based on a groundbreaking concept developed by Endo et al. for the synthesis of a carboranyl analogues of estradiol (*31*, *32*). Analogous to Endo's carboranyl estradiols, both the B and the C ring of cholesterol were replaced with a carborane cluster in the boronated cholesterol mimics described in this paper (Figure 1). The design and synthesis of these structures, their incorporation into liposomes, and the evaluation of the capacity of these liposomes for efficient boron delivery are the subjects of this paper. Both the folate receptor (FR) (*33*, *34*) and the vascular endothelial growth factor receptor-2 (VEGFR-2) (*35*, *36*) have been identified as important molecular targets for cancer therapy in recent years. The capacity of the designed boronated liposomes for incorporation of receptor-targeting ligands such as folate and VEGF (vascular endothelial growth factor) and the results of in vitro uptake and cytotoxicity studies with the resulting constructs are discussed.

EXPERIMENTAL PROCEDURES

General Chemical Procedures. Proton and carbon-13 NMR spectra were obtained on Bruker (250 MHz or 400 MHz) NMR instruments at The Ohio State University College of Pharmacy. Chemical shifts are reported in parts per million (ppm) from an internal tetramethylsilane standard. The coupling constants are reported in hertz (Hz). High resolution electron impact mass spectrometry (HR-EIMS) was carried out with a Kratos MS-25 instrument with typical ionization conditions of 70 eV electron impact ionization at the Department of Chemistry of The Ohio State University by Dr. Christopher M. Hadad and Ms. Susan Hatcher. Compound visualization on silica gel 60 F_{254} precoated TLC plates (0.25 mm layer thickness) (Merck, Darmstadt, Germany) was attained by UV light. Carborane-containing compounds were selectively visualized by spraying a solution of 0.06% $PdCl_2$/1% aqueous HCl on TLC plates and subsequent heating to ∼120 °C, which caused the slow formation (15−45 s) of gray spots due to the reduction of Pd^{2+} to Pd^0. Reagent-grade solvents were used for column chromatography using silica gel 60, particle size 0.040−0.063 mm (Merck, New Jersey). Standard chemicals were purchased from various vendors. *Para*- and *meta*-carborane were purchased from Katchem, Prague, Czech Republic. All chemicals were used as purchased without further purification. Anhydrous benzene, anhydrous dichloromethane, and anhydrous tetrahydrofurane (THF) were purchased from VWR Scientific Products. THF was additionally dried over sodium metal before use. All chemical syntheses were carried out under argon atmosphere to maintain inert reaction condition unless mentioned otherwise.

1-(4-Methoxyphenyl)-7-(6-methylheptyl)-1,7-dicarba-*closo*-dodecaborane (2). To a solution of 1-(4-methoxyphenyl)-1,7-dicarba-*closo*-dodecaborane (*31*) (**1**) (125 mg, 0.5 mmol) in THF (20 mL) at 0 °C was added *n*-BuLi (2.5 M in hexane, 0.2 mL, 0.51 mmol). The mixture was first stirred at 0 °C for 45 min and then for 1 h at room temperature. Toluene-4-sulfonic acid 6-methylheptyl ester (*37*) (142 mg, 0.5 mmol) in 5 mL THF was added and the resulting mixture stirred for 12 h at room temperature, poured into ice−water (50 mL), extracted with ether (3 × 50 mL), washed with brine, and dried over $MgSO_4$. The solvent was evaporated under vacuum, and the residue was purified by silica gel flash column chromatography using hexanes/ethylacetate (9:1) as the eluent (TLC R_f: 0.5) to give **2** in 61% yield. ^{1}H NMR ($CDCl_3$): δ 0.83−0.85 (d, 6H, J = 6.5 Hz) 1.15−1.38 (m, 9H, CH_2), 2.16 (2H, t, J = 6 Hz), 3.75 (s, 3H), 6.64−6.67 (2H, d, J = 8.6 Hz), 7.51−7.55 (2H, d, J = 8.6 Hz). ^{13}C NMR ($CDCl_3$): δ 19.59, 23.01, 27.40, 28.31, 29.86, 30.12, 30.45, 37.59, 39.20, 54.89, 55.72, 72.23, 113.89, 128.19, 129.39, 160.14. HR-EIMS calcd for $C_{17}H_{34}B_{10}O$ (M^+): 362.3607. Found 362.3585.

1-(4-Methoxyphenyl)-12-(6-methylheptyl)-1,12-dicarba-*closo*-dodecaborane, an intermediate in the synthesis of compound **II**, was obtained by adapting the procedure described for compound **2** using 1-(4-methoxyphenyl)-1,12-dicarba-*closo*-dodecaborane (*31*) as the starting material. Purification by silica gel flash chromatography using hexanes/ethylacetate (9:1) as the eluent (TLC R_f: 0.5) gave 1-(4-methoxyphenyl)-12-(6-methylheptyl)-1,12-dicarba-*closo*-dodecaborane in 52% yield. ^{1}H NMR ($CDCl_3$): δ 0.82−0.84 (d, 6H, J = 6.6 Hz) 1.20−1.39 (m, 9H, CH_2), 2.15 (t, 2H, J = 6.5 Hz), 3.75 (s, 3H), 6.75−6.72 (d, 2H, J = 7.5 Hz), 7.32−7.29 (d, 2H, J = 7.5 Hz). ^{13}C NMR ($CDCl_3$): δ 23.01, 27.40, 28.31, 29.86, 30.12, 30.45, 37.60, 39.20, 55.72, 72.25, 113.64, 113.90, 116.75, 128.58, 129.39, 129.73, 138.59, 159.95. HR-EIMS calcd for $C_{17}H_{34}B_{10}O$ (M^+): 362.3607. Found: 362.3585.

1-(3-Methoxyphenyl)-12-(6-methylheptyl)-1,12-dicarba-*closo*-dodecaborane, an intermediate in the synthesis of compound **III**, was obtained by adapting the procedure described for compound **2** using 1-(3-methoxyphenyl)-1,12-dicarba-*closo*-dodecaborane (*31*) as the starting material. Purification by silica gel flash chromatography using hexanes/ethylacetate (9:1) as the eluent (TLC R_f: 0.5) gave the 1-(3-methoxyphenyl)-12-(6-methylheptyl)-1,12-dicarba-*closo*-dodecaborane in 55% yield. ^{1}H NMR ($CDCl_3$): δ 0.82−0.84 (d, 6H, J = 6.6 Hz) 1.11−1.39 (9H, m, CH_2), 1.97 (t, 2H, J = 8.3 Hz), 3.64 (3H, s), 6.71−6.75 (dd, 2H, J = 10 Hz), 7.29 (s, 1H), 7.32−7.31(d, 1H, J = 2.2 Hz). ^{13}C NMR ($CDCl_3$): δ 24.3, 28.10, 29.20, 30.02, 31.03, 32.24, 40.12, 50.10, 115.20, 113.89, 128.20, 129.25, 129.39,

160.15. HR-EIMS calcd for $C_{17}H_{34}B_{10}O$ (M^+): 362.3607. Found: 362.3585.

1-(4-Hydroxyphenyl)-7-(6-methylheptyl)-1,7-dicarba-*closo*-dodecaborane (I). To a solution of 1-(4-methoxyphenyl)-7-(6-methylheptyl)-1,7-dicarba-*closo*-dodecaborane (**2**) (90.5 mg, 0.25 mmol) in CH_2Cl_2 (5 mL) was added dropwise a 1 M solution of BBr_3 in CH_2Cl_2 (0.48 mL) at −78 °C. The mixture was stirred at room temperature for 2 h, then poured into ice water and extracted with CH_2Cl_2. The organic layer was washed with brine, dried over Na_2SO_4, and concentrated under vacuum. Purification by silica gel flash chromatography (hexanes/ethylacetate 8:2; R_f: 0.4) gave **I** in 56% yield. ^{1}H NMR ($CDCl_3$): δ 0.87−0.85 (d, 6H, J = 7.9 Hz), 1.10−1.64 (m, 9H, CH_2), 1.98 (t, 2H, J = 8.2 Hz), 6.68−6.70 (d, 2H, J = 8.6 Hz), 7.78−7.80 (d, 2H, J = 8.0 Hz). ^{13}C NMR ($CDCl_3$): δ 23.01, 27.40, 28.316, 29.86, 30.12, 30.45, 37.59, 39.20, 81.12, 86.41, 115.38, 128.50, 129.65, 156.181. HR-EIMS calcd for $C_{16}H_{32}B_{10}O$ (M^+): 348.3450. Found: 348.3453.

1-(4-Hydroxyphenyl)-12-(6-methylheptyl)-1,12-dicarba-*closo*-dodecaborane (II) was obtained by adapting the procedure described for compound **I** using 1-(4-methoxyphenyl)-12-(6-methylheptyl)-1,12-dicarba-*closo*-dodecaborane as the starting material. Purification by silica gel flash chromatography (hexanes/ethylacetate 8:2; R_f: 0.4) gave **II** in 50% yield. ^{1}H NMR ($CDCl_3$): δ 0.82−0.85 (d, 6H, J = 6.5 Hz), 1.09−1.36 (m, 9H, CH_2), 1.97 (2H, t, J = 8.0 Hz), 6.65−6.68 (d, 2H, J = 8.7 Hz), 7.24−7.28 (d, 2H, J = 8.7 Hz), ^{13}C NMR: δ 23.01, 26.37, 27.40, 28.31, 28.62, 29.86, 30.12, 30.54, 32.34, 34.09, 66.64 72.26, 128.29, 128.50, 129.65, 156.17. HR-EIMS calcd for $C_{16}H_{32}B_{10}O$ (M^+): 348.3450. Found: 348.3454.

1-(3-Hydroxyphenyl)-12-(6-methylheptyl)-1,12-dicarba-*closo*-dodecaborane (III) was obtained by adapting the procedure described for compound **I** using 1-(3-methoxyphenyl)-12-(6-methylheptyl)-1,12-dicarba-*closo*-dodecaborane as the starting material. Purification by silica gel flash chromatography (hexanes/ethylacetate 8:2; R_f: 0.4) gave **III** in 46% yield. ^{1}H NMR ($CDCl_3$): δ 0.82−0.84 (d, 6H, J = 6.6 Hz) 1.11−1.39 (m, 9H, CH_2), 1.99 (t, 2H, J = 8.3 Hz), 6.70−6.74 (dd, 2H, J = 10 Hz), 7.29 (s, 1H), 7.30−7.31 (d, 1H, J = 2.2 Hz). ^{13}C NMR ($CDCl_3$): δ 22.59, 26.97, 27.90, 29.45, 30.03, 37.20, 38.80, 68.54, 77.87, 114.98, 129.24, 134.07, 135.21, 145.10, 165.02. HR-EIMS calcd for $C_{16}H_{32}B_{10}O$ (M^+): 348.3450. Found: 348.3453.

RMS Fit of Cholesterol with Compounds I−III (Figure 2). *Hyperchem 7.51* (Hypercube, Inc., Gainsville, FL) was used on a Dell Inspiron 4100 to produce the rms fit of cholesterol with the carboranyl cholesterol mimics **I**−**III**. Carboranyl cholesterols **I**−**III** were energy-minimized with the HyperMMplus module, using the Polak−Ribiere conjugate gradient method and an energy gradient of 0.03 kcal mol^{-1} Å^{-1}. The minimized structures of **I**−**III** were then used for the rms fit with the energy-minimized structure of cholesterol. Appropriate side-chain carbons were used to obtain the optimal fit.

Polar and Apolar Surface Areas (PSAs/APSAs) of Cholesterol and Compounds I−III (Table 1). Parameters for minimized structures, generated as described in the previous section, were transferred to the *VEGA ZZ 2.0.4* software package (*38*) for the calculation of PSAs and APSAs. Analogous to previous theoretical studies involving carborane-containing compounds (*39*, *40*), boron atom types in the carborane clusters of compounds **I**−**III** were replaced with carbon atom types using *Hyperchem 7.51* before data transfer to *VEGA ZZ 2.0.4*.

Calculated LogP Values of Cholesterol and Compounds I−III (Table 1). LogP calculations were carried out using the *ChemDraw 7.0.1* version (CambridgeSoft Corporation, Cambridge, MA). This software package does not allow LogP calculations with compounds containing hexavalent boron and/or carbon atoms, as they can be found in the carborane cluster. Therefore, the carborane clusters in compounds **I**−**III** (Figure 1) were replaced with adamantane, because both cage structures are comparable in lipophilicity and dimensions (*41*). In order to mimic para and meta substitution patterns in compounds **I**−**III**, the 1,4(6,10)-position and 1,3(5,7)-position of the adamantane moiety were substituted appropriately. For validation, experimental LogP values of a series of twelve previously described carboranyl compounds (*42*) and the calculated LogP values of their virtual adamantane counterparts were fitted on a straight line to obtain the R^2 value. The obtained R^2 value of 0.92 indicated that the approximation of using adamantane instead of the carborane moiety for the theoretical calculation of the LogP values of carboranyl compounds with *ChemDraw* is acceptable.

Materials for Biological Studies. Dipalmitoylphosphatidylcholine (DPPC) was purchased from Genzyme (Boston, MA). Monomethoxypolyethylene glycol(2000)−distearoylphosphati-

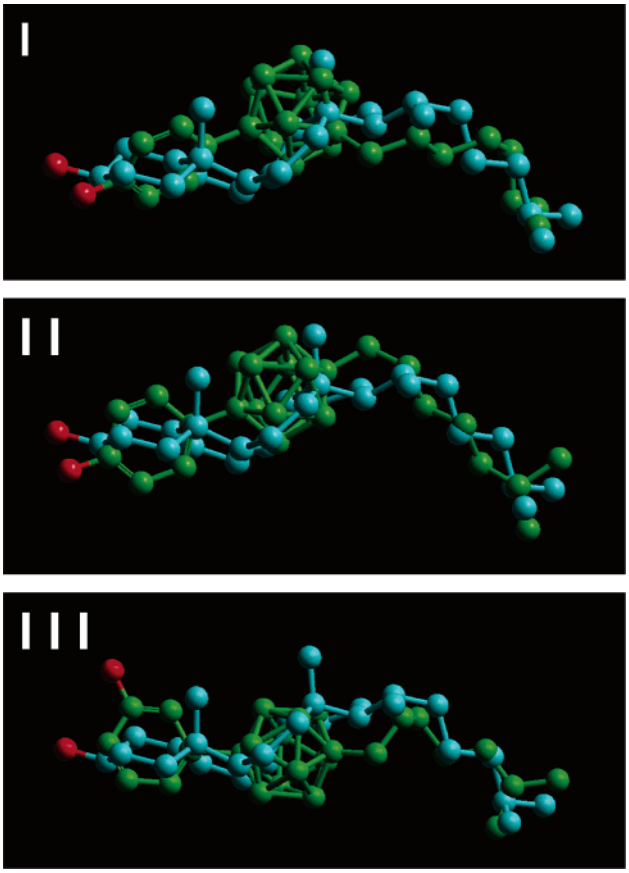

Figure 2. RMS fit of cholesterol with compounds **I**−**III**. Hydrogen atoms were omitted for the clarity. Cholesterol is shown in cyan and compounds **I**−**III** in green. For better orientation, oxygen atoms of all molecules are shown in red.

Table 1. Calculated LogPs,[a] Apolar Surface Areas (APSAs),[a] Polar Surface Areas (PSAs),[a] and APSA/PSA Ratios of Cholesterol and Compounds I−III

Compd.	LogP	APSA (Å^2)	PSA (Å^2)	Ratio APSA/PSA
Chol[b]	7.35	504.4	29.0	17.4
I	7.12	492.4	33.2	14.8
II	7.26	468.8	32.8	14.3
III	7.26	467.0	29.2	15.9

[a] See Experimental Procedures ("Calculated LogP Values of Cholesterol and Compounds I-III" and "Polar and Apolar Surface Areas (PSAs/APSAs) of Cholesterol and Compounds I-III") for detailed descriptions. [b] Cholesterol [experimental LogP: 7.445 (http://redpoll.pharmacy.ualberta.ca/drugbank)].

dylethanolamine (mPEG−DSPE) was purchased from Lipoid (Newark, NJ). Distearoylphosphatidylethanolamine−polyethylene glycol(2000)−maleimide (DSPE−PEG(2000)−maleimide) was purchased from Avanti Polar Lipids, Inc. (Alabaster, AL). Cholesterol, calcein, and Sepharose CL-4B were purchased from Sigma (St. Louis, MO). Folate−polyethylene glycol-(2000)−cholesterol (folate−PEG−cholesterol) was synthesized as described previously (*43*). Spectra/Por DispoDialyzer dialysis tubes (1 mL, molecular weight cutoff [MWCO] 10 000) were purchased from Spectrum Lab (Rancho Dominguez, CA). Tissue culture media RPMI 1640 without folic acid, fetal bovine serum (FBS), and antibiotics were purchased from Life Technologies (Rockville, MD). The KB HeLa variant cell line (ATCC # CCL-17) was gift from Dr. Philip Low, Purdue University (West Lafayette, IN). The 293/KDR cell line, expressing 2.5×10^6 VEGFR-2/cell, has been described in detail previously by us (*44*). Nitric acid (trace metal quality) was purchased from Fisher Scientific (Pittsburgh, PA) and 18.2 MΩ−cm water was obtained from a Milli-Q laboratory purification unit (Millipore, Billerica, MA). Other materials and vendors are listed in the following: Mouse antihuman VEGF monoclonal antibody (Pharmingen, San Diego, CA); Anti-mouse IgG: horseradish peroxidase (HRP) conjugate (GE Healthcare, Piscataway, NJ), Enhanced Chemiluminescent (ECL) Plus kit (GE Healthcare, Piscataway, NJ), Anti-phosphotyrosine RC20 antibody conjugated to horseradish peroxidase (BD Transduction Labs, San Diego, CA), SLT (Shiga-like toxin)−VEGF (SibTech, Newington, CT), CellTiter 96 AQ_{ueous} One Solution Cell Proliferation Assay kit (Promega, Madison, WI).

Preparation of Liposomes. Nontargeted liposomes, control liposomes, and FR-targeted liposomes were prepared using the thin-layer evaporation method (*45*). The particle size was reduced by ultrasonication and extrusion. The compositions for each liposomal formulation were as follows: Nontargeted liposome (DPPC/compound **I**/mPEG−DSPE, 55:40:5 mol %), control liposome (DPPC/cholesterol, 55:45 mol %), and FR-targeted liposome (DPPC/compound **I**/mPEG−DSPE/folate−PEG−cholesterol, 55:40:4.5:0.5 mol %). Lipids were first dissolved in chloroform, dried to a thin film in a round-bottom flask under nitrogen, and then further dried using vacuum for 4 h. The dried lipid was then resuspended using 10 mM calcein solution and pulse-sonicated for 5 min. The resulting liposomal suspension was passed through a 100 nm polycarbonate membrane for five cycles using a high-pressure extruder (Northern Lipid, Vancouver, British Columbia, Cannada). A 10 mL Sepharose CL-4B column equilibrated with pH 7.4 phosphate buffered saline (PBS) was applied to separate the liposomal portions from low molecular weight components. Elutions were collected in 1 mL quantities and subjected to the determination of boron concentrations by inductively coupled plasma atomic emission spectroscopy (ICP-AES) as described in a following section on boron measurements.

(VEGFR-2)-targeted liposomes were prepared as follows: Cys-tagged single-chain VEGF (scVEGF) was constructed and expressed, as described previously (*46*). Briefly, two 3−112 aa long fragments of human $VEGF_{121}$ were fused head-to-tail and expressed with a N-terminal Cys-tag, a novel cysteine-containing 15-aa peptide tag for site-specific modification of recombinant proteins (*47*). scVEGF was site-specifically lipidated with DSPE−PEG(2000)−maleimide and incorporated into liposomes as follows: scVEGF was incubated with DSPE−PEG(2000)−maleimide at a molar protein to lipid ratio of 1:10 at ambient temperature for 2 h, then mixed with an equal volume of the nontargeted liposomal formulation of compound **I** described above and incubated at 37 °C for 16 h. Non-incorporated scVEGF was removed by chromatography on Sepharose CL-4B. Purified VEGF/liposomes were analyzed by Western blotting using mouse antihuman VEGF monoclonal antibody diluted 1:2000 followed by anti-mouse IgG−HRP conjugate diluted 1:10 000. The anti-VEGF antibody was visualized on the blots by the ECL Plus kit.

In Vitro Release Analysis of Liposomes. The in vitro release profiles of nontargeted liposomes, control liposomes, and FR-targeted liposomes were measured by both calcein release and determination of boron concentrations via ICP-AES. Briefly, 1 mL of Sepharose CL-4B column-purified liposome samples were added to 1 mL dialysis tubes (MWCO 10 000) and incubated in 500 mL PBS at 37 °C. Constant magnetic stirring (100 rpm) was applied to the dialysis beaker. At 24, 48, 72, and 96 h, 1 mL samples were taken from the beaker, and the released calcein was measured using a Perkin-Elmer spectrofluorometer (Wellesley, MA) with excitation and emission at 485 and 520 nm, respectively. Excitation and emission slits were set to 5 nm. The boron concentrations of liposomal suspensions before and after the dialysis were also measured by ICP-AES. The percentage of retention was calculated on the basis of normalization using the original concentration before dialysis.

Boron Uptake Study of Liposomes in FR-Positive KB Cells. KB cells were cultured as a monolayer in folate-free Roswell Park Memorial Institute (RPMI) 1640 media supplemented with penicillin, streptomycin, and 10% FBS in a humidified atmosphere containing 5% CO_2 at 37 °C. After reaching confluence, KB cells were collected with trypsin/ethylenediaminetetraacetic acid (EDTA), washed with PBS, and suspended in folate-free RPMI media at a density of 2×10^7 cells/mL. Boronated FR-targeted or nontargeted liposomes (40 μg/mL boron) were added to the media, and cells were incubated under CO_2 atmosphere at 37 °C for 2 h. Subsequently, cells were centrifuged at 400 g for 10 min, and the media was removed. Cells were washed twice with cold PBS by resuspension and centrifugation at 400 g. Cell pellets were then collected, and boron concentrations were determined by direct current plasma-atomic emission spectroscopy (DCP-AES) (*48*). All treatments and measurements were triplicated.

Functional Activity of (VEGFR-2)-Targeted Liposomal Formulations of Compound I. The functional activity of VEGF inserted into nontargeted liposomal formulations of compound **I** (see Preparation of Liposomes section) was evaluated in tissue culture using 293/KDR cells expressing 2.5×10^6 VEGFR-2/cell. Two functional assays, VEGFR-2 tyrosine autophosphorylation and protection of 293/KDR cells from VEGFR-2 mediated toxicity of the SLT−VEGF chimeric toxin, were carried out as described previously by us (*49*). Briefly, for VEGFR-2 autophosphorylation, 7.5×10^4 293/KDR cells were plated into 24-well plates. After 6 h, complete medium (Dulbecco's Modified Eagle Medium [DMEM]/10% FBS) was replaced with starvation medium (DMEM/0.5% FBS) and the cells were incubated for 16 h at 37 °C in 5% CO_2. Subsequently, the starvation medium was replaced with serum-free DMEM containing 0.5 mM sodium vanadate for 20 min at 37 °C; the cells were incubated with VEGF-2 or (VEGFR-2)-targeted liposomes for 10 min at 37 °C, lysed, and analyzed by Western blotting using anti-phosphotyrosine RC20 antibody conjugated to horseradish peroxidase. For the SLT−VEGF protection assay, 10^3 293/KDR cells were plated on 96-well plates. Varying amounts of (VEGF-2)-targeted liposomes were mixed with SLT−VEGF in complete medium (DMEM/10% FBS) and added to cells in triplicate wells to a final SLT−VEGF concentration of 1 nM. Cells were quantitated after 96 h incubation using a CellTiter 96 AQ_{ueous} One Solution Cell Proliferation Assay kit.

Transmission Electron Microscope (TEM) and Photon Correlation Spectroscopy (PCS) Analysis. The consistencies of nontargeted liposomes, control liposomes, and FR-targeted

liposomes constructed with compound **I** were investigated with TEM after negative staining with uranyl acetate (UA) as described previously (*50*). Briefly, the liposomal samples were placed onto 100-mesh grids. After 3 min, excess solution was wiped off with filter paper, and the grid was immersed in 2% UA. The UA solution was removed after 1 min, and the grids were washed twice with 200 μL of distilled water. The grids were then imaged on a Philips CM 12 transmission electron microscope (Campus Microscopy and Imaging Facility, OSU, Columbus, OH). Photos were taken at 55 000-fold magnification from the suspended liposomal particles. The mean particle diameter and distribution were measured by PCS on a NICOMP particle sizer model 370 (Santa Barbara, CA), and the normalized Gaussian-distributed volume-weighted particle size was collected after 3 runs.

Boron Determinations. Boron concentrations of samples obtained from boron uptake studies with KB cells were obtained by DCP-AES, as described previously (*48*). Boron concentrations for all other samples were obtained by ICP-AES with a Varian VISTA AX ICP spectrometer system. The Varian argon-purged echelle spectrometer, which has a bandpass of $\leq$10 pm at wavelengths below 260 nm, enabled intensity measurements free of spectral interferences for the four neutral-atom boron lines used in this study: 208.889 nm, 208.956 nm, 249.678 nm, and 249.772 nm. All relative intensities for boron spectral lines were based on background-corrected peak heights. A charge-coupled device (CCD) detector, maintained at −34 °C by a Peltier cooler, generated all spectrum-based electronic signals processed by the spectrometer system. The central axial region of a 1.3 kW, 40 MHz ICP was aligned optically with the axis of the acceptance angle of the Echelle spectrometer. Sample solutions were injected into the high-temperature plasma as aerosols produced by a perfluoroalkoxy (PFA) nebulizer. The aerosols first passed through a 50 mL Polycon cyclone spray chamber from which fine aerosol particles were swept by an argon stream through a polytetrafluoroethylene (PTFE) tube and alumina injector tube into the plasma. In the plasma, free atoms and ions were produced and excited to emit quantized radiation. Calibration was achieved with one blank and four accurately diluted aliquots of a single-element standard solution. The boron concentration in the original standard was certified traceable to the National Institute of Standards and Technology (NIST) by the supplier, Inorganic Ventures (Lakewood, NJ). All dilutions, including those for samples, were accomplished in polyethylene tubes on a mass basis enabled by an analytical balance capable of measurements to 0.1 mg. The diluent was 0.5 M nitric acid in 18.2 MΩ−cm water. Samples (1 mL) were diluted by factors that ranged from 3 to 15 to provide the 3 mL solution volume needed for nebulization into the ICP. Calibration functions were second-degree polynomial least-square regression fits with correlation coefficients greater than 0.995. Concentration values obtained by this approach generally are within 10% of actual concentrations. Certified reference materials were not available for further corroboration of accuracy.

RESULTS AND DISCUSSION

Design of Carboranyl Cholesterol Mimics. As already discussed in the Introduction, the design strategy for carboranyl cholesterol mimics described in this paper is based on the a replacement of the B and C rings of cholesterol with highly lipophilic *meta*- and *para*-carborane clusters (*31*, *32*). The dimensions of these clusters are approximately 50% larger than the space occupied by the three-dimensional sweep of a phenyl group (*51*). Figure 1 shows the structural resemblance of cholesterol and the carboranyl cholesterols mimics **I**−**III**. In order to further validate our design strategy, we calculated apolar and polar surface areas (APSAs, PSAs) as well as the LogP values of all compounds shown in Figure 1 prior to embarking on the synthesis of compounds **I**−**III**. Using *HyperChem 7.51* software, we also produced an overlay of energy-minimized structures of compounds **I**−**III** with that of cholesterol. The data are summarized in Figure 2 and Table 1. In particular, the structures of compounds **I** and **II** showed very good structural overlap with the structure of cholesterol, and APSAs, PSAs, and LogP values of all compounds were similar.

Scheme 1. Representative Synthesis of Carboranyl Cholesterol Mimics Using Compound I as the Example[a]

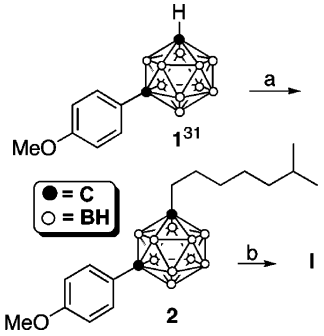

[a] Key: a, *n*-BuLi/toluene-4-sulfonic acid 6-methylheptyl ester/benzene/room temperature; b, BBr_3/CH_2Cl_2, room temperature.

Synthesis of Carboranyl Cholesterol Mimics. Encouraged by our computational studies, we carried out the syntheses of compounds **I**−**III** as shown in Scheme 1 by the example of compound **I**. Starting material for the synthesis of compound **I** was 1-(4-methoxyphenyl)-1,7-dicarba-*closo*-dodecaborane (Scheme 1, compound **1**), which was previously described by Endo et al. (*31*). For the syntheses of compounds **II** and **III**, 1-(4-methoxyphenyl)- (*31*) and 1-(3-methoxyphenyl)-substituted *para*-carborane (*31*), respectively, were used as starting materials. Compound **1** was reacted with toluene-4-sulfonic acid 6-methylheptyl ester (*37*) to afford compound **2**. The yields for compound **2** and its derivatives used in the syntheses of **II** and **III** ranged from 52% to 61%. The methoxy group in **2** was removed using boron tribromide in dichoromethane to afford target compound **I**. Target compounds **II** and **III** were obtained in a similar fashion, and yields for all three target compounds ranged from 46% to 56%. All intermediates and target compounds were purified effectively by silica gel column chromatography and characterized by ^{1}H NMR, ^{13}C NMR, and HR-EIMS. An important criterion for the synthesis of compounds **I**−**III** was practicability. All target compounds were synthesized from readily available starting materials. However, structural resemblance of carboranyl cholesterol mimics with cholesterol probably could be further improved by substituting the A ring of cholesterol with nonaromatic ring systems instead of using the phenyl group (*52*), methyl substitution at boron atoms of the carborane clusters (*53*), and insertion of a 2,6-dimethylheptane (*54*) rather than a 6-methylheptane side chain. However, such a structure would require multiple laborious reaction steps. It should be noted that, due to the high lipophilicity of all carboranyl compounds described in this paper, standard ESI-MS (electrospray ionization mass spectrometry) was unsuccessful, and EIMS had to be used.

Incorporation of Carboranyl Cholesterol Mimics into Liposomes. Compounds **I**−**III** were formulated into nontargeted liposomes using the thin-layer evaporation method (*10*), and the particle sizes and lamellarities were further defined using ultrasonication followed by extrusion. We characterized the incorporation efficiency using size-exclusion chromatography. Liposomal and free compound fractions were separated at different elution volumes, and the boron concentrations were measured by ICP-AES. The results, shown in Figure 3, indicated

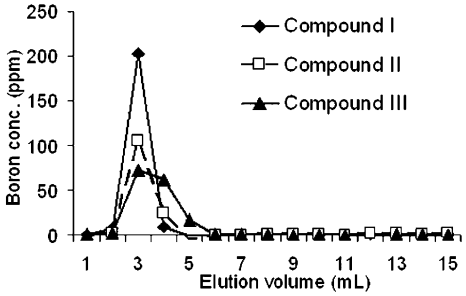

Figure 3. Incorporation of compounds **I**−**III** into liposomes. The preparation for the liposomes are described in Experimental Procedures (composition = DPPC/compound **I**−**III**/PEG−DSPE, 55:40:5 mol %). Encapsulation of boron compounds was determined by eluting 0.5 mL liposomal samples through a 10 mL Sepharose CL-4B column with pH 7.4 PBS. Fractions were collected for determination of boron concentrations by ICP-AES. The encapsulation efficiencies were 99.7% for compound **I**, 94.3% for compound **II**, and 96.8% for compound **III**.

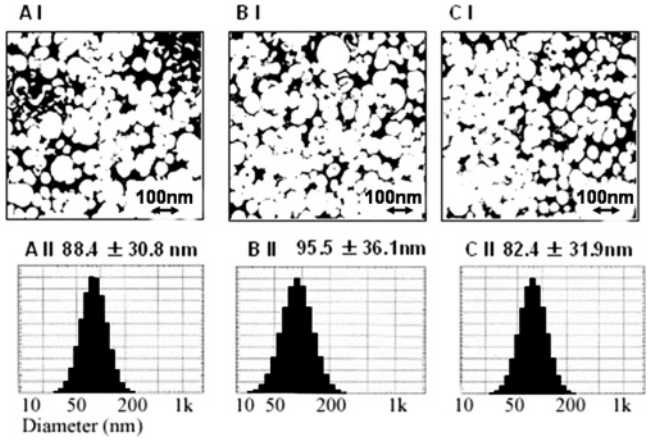

Figure 4. Characterization of size distribution and lamellarity of liposomal formulations of compound **I**. (A) nontargeted boronated liposome; (B) non-boronated control liposome (DPPC/cholesterol); (C) FR-targeted boronated liposome. (I) Morphology of the liposomes visualized by transmission electronic microscopy (TEM). Negative staining was applied to observe the particle size and lamellarity of liposomes. Formation of small unilamellar vesicle (SUV) was confirmed for all three formulations of compound **I**. (II) Particle sizes measured by photon correlation method. Numbers shown are the mean particle size ± standard deviation (volume-weighted) of the individual samples.

that all three compounds had >90% incorporation efficiency (**I** = 99.7%, **II** = 94.3%, and **III** = 96.8%). For all liposomal formulations prepared subsequently from compound **I** for in vitro release and cell uptake studies, >90% incorporation efficiency was confirmed with the same method (data not shown). Samples for in vitro release and cell uptake studies were all purified using the Sepharose CL-4B column to eliminate free compound. Compound **I** was selected for all further studies because of its good structural overlap with cholesterol (Figure 2) and its high incorporation efficiency.

Size and Lamellarity Characterization of Liposomal Formulations of Compound I. For liposomal delivery of BNCT agents, as well as other anticancer therapeutics, the size distribution and lamellarity of liposomes are of great importance for parameters such as stability, drug release profile, in vivo half-life, and tissue distribution. Small, homogeneous, and unilamellar particles are preferred for optimal delivery to malignant tissues, as they are able to escape reticular endothelial system (RES) uptake (*55*). We applied TEM and PCS for the analysis of the physical properties of conventional, nontargeted, and FR-targeted liposomes. After negative staining, both FR-targeted and nontargeted liposomal formulation of compound **I** were inspected with TEM (Figure 4AI,CI) for particle size distribution and lamellarity observation. As a control, conventional liposomes (DPPC/cholesterol [55:45 mol %]) were also constructed under identical conditions and analyzed accordingly (Figure 4BI). Since the TEM method does not allow the particle size quantification, the same samples were also analyzed for mean particle size and distribution using a laser particle sizer in parallel (Figure 4AII,CII). Data presented in Figure 4 demonstrate that homogeneous small unilamellar vesicles (SUVs) were formed by using compound **I** both for nontargeted and FR-targeted liposomal formulations. The mean particle sizes for all three formulations ranged from 82.4 to 95.5 nm with size distributions around 30−40 nm. No major differences were found in appearance, size distribution, and lamellarity between conventional DPPC/cholesterol liposomes, nontargeted, and FR-targeted liposomal formulations of compound **I**.

In Vitro Release of Liposomal Formulations of Compound I. The performance of boron-containing liposomes in vivo is highly affected by the stability of incorporation of the boron entities. Therefore, a standard in vitro release experiment (*56*) was conducted using PBS as the media at 37 °C, and the stability of incorporation of compound **I** in both FR-targeted and nontargeted liposomal formulation was evaluated. Control liposomes were constructed with cholesterol instead of compound **I**, and thus, calcein, a green fluorescent dye, was encapsulated into the liposomal hydrophilic compartment of all liposomal formulations to analyze stability via fluorescence measurements of calcein release. Samples were taken at different time points beginning at 0.5 h after the initiation of incubation, and calcein release was measured by absorbance (Figure 5A). Boron concentrations of samples obtained at 0 and 96 h were determined by ICP-AES (Figure 5B). Overall, both data sets indicate that a 45% molar ratio of compound **I** was stably incorporated into the vesicles and that the release of calcein followed a pattern similar to that of conventional DPPC−cholesterol liposomes. For both the nontargeted and FR-targeted formulation, the calcein release was less than 30% at 24 h, which was not significantly different from the control liposome. At later time points, however, the targeted formulation appeared to release calcein, and presumably also boron, at an increased rate. This could be due to insufficient anchoring of folate−PEG−cholesterol to the lipid bilayer or even the degradation of this receptor-targeting ligand. We have made similar observations previously in studies using doxorubicin as the incorporated compound (X.B. Zhao, unpublished results). Nevertheless, nontargeted liposomal formulations showed a release profile comparable to that of the control liposomes, with more than 50% calcein and boron remaining unreleased at 96 h. The release rate of FR-targeted liposomes at least until 48 h should be sufficient for selective receptor-mediated boron delivery to tumor cells for BNCT.

In Vitro Uptake of FR-Targeted Liposomal Formulations of Compound I. We determined the in vitro delivery of compound **I** to KB cells, an established FR-expressing cell line (*57*), in the form of nontargeted liposomal formulations as well as in FR-targeted liposomal formulations in the presence and absence of free 5 mM free folate. No significant cytotoxicity was noted during the 4 h incubation time based on a microscopic inspection of the cells. Cellular uptake of the liposomes was determined by measuring cell-associated boron concentrations with DCP-AES (*48*). The obtained data are summarized in Figure 6. The nontargeted liposomal formulation of compound **I** appeared to bind in a nonspecific way to KB cells (30 μg boron/g cells), which have a very low background level of boron (<1 μg boron/g cells; data not shown) in cell culture environment. Specific targeting to FR was demonstrated by increased boron levels for FR-targeted liposomal formulation of compound

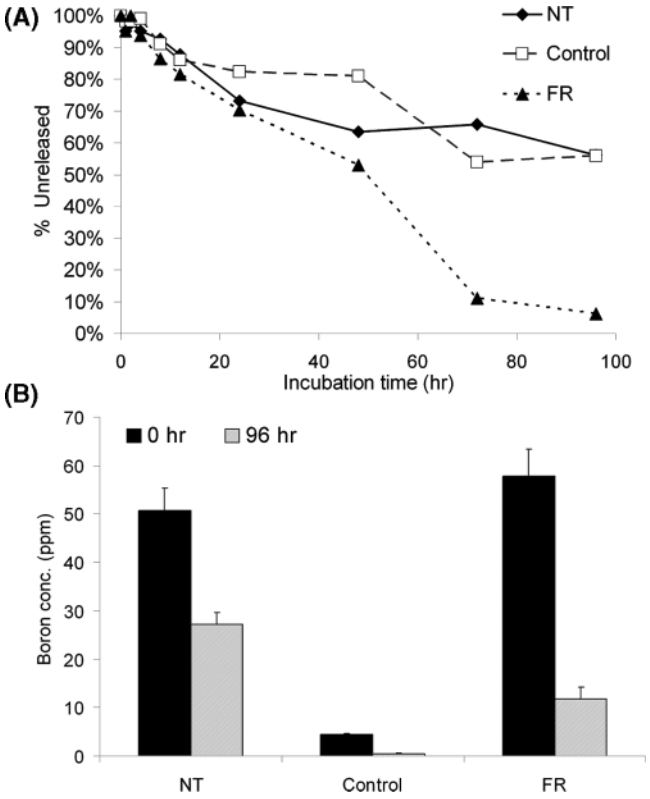

Figure 5. In vitro release profile of liposomal formulations of compound **I** in pH 7.4 PBS at 37 °C. (A) Compound **I** was formulated into liposomes with different compositions as described in Experimental Procedures. In parallel, DPPC/cholesterol control liposomes without boron components were prepared using the same protocol. All liposomal formulations contain a 10 mM solution of calcein. The percentage of calcein release was determined by fluorescence and absorbance measurements. (B) Boron concentrations of the liposomal suspensions were measured at 0 and 96 h by ICP-AES. NT: boronated liposomes (nontargeted). Control: control liposomes (no boron). FR: FR-targeted boronated liposomes. Error bars shown in Figure 5B are based on standard deviations calculated from three measurements.

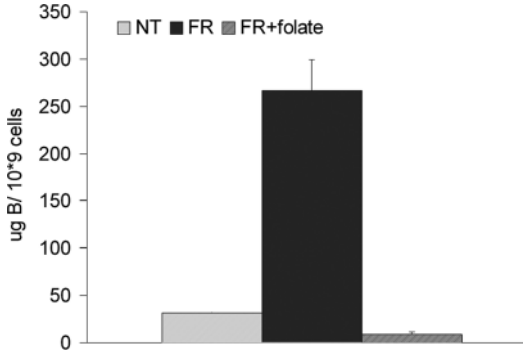

Figure 6. Cellular uptake of liposomal formulations of compound **I**. NT: Nontargeted boronated liposomes. FR: FR-targeted boronated liposomes. FR + folate: FR-targeted boron-containing liposomes were coincubated with 5 mM free folate. 2×10^7 cells in 1 mL media were incubated with liposomes containing 40 μg/mL boron. Each data point represents the mean of boron amount in the cell lysates normalized to 1×10^9 cells (equivalent to 1 g tissue). Error bars stand for standard deviations of the normalized boron amount in triplicates.

I (267 μg/g cells). FR specificity was further demonstrated by the reduction of the boron concentration of FR-targeted boronated liposomes that were incubated with KB cells in the presence of 5 mM free folate (9 μg/g cells). All three liposomal formulations were colabeled with calcein, and specific binding was also confirmed by the increased fluorescence intensity in KB cells treated with FR-targeted boronated

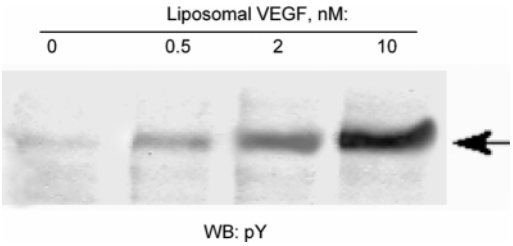

Figure 7. (VEGFR-2)-targeted liposomes induce VEGFR-2 autophosphorylation in a dose-dependent manner. 293/KDR cells were stimulated with the indicated concentrations of liposomal scVEGF, and tyrosine phosphorylation of VEGFR-2 was determined by Western blotting with an anti-phosphotyrosine RC20−HRP conjugate. The arrow indicates the position of VEGFR-2.

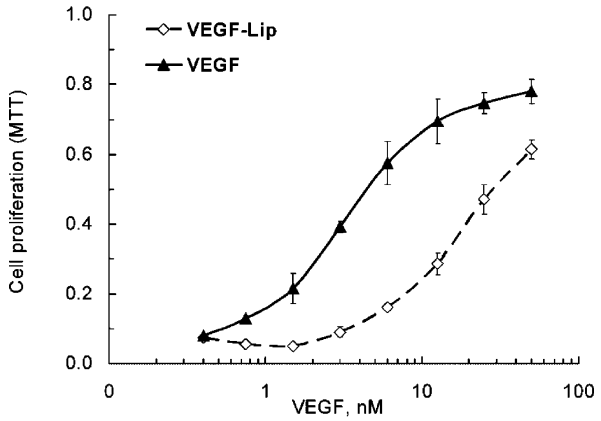

Figure 8. Boronated (VEGFR-2)-targeted liposomes protect VEGFR-2 expressing 293/KDR cells from SLT−VEGF-induced cell death. 293/KDR cells were exposed to boronated (VEGFR-2)-targeted liposomes (VEGF-Lip) or scVEGF (VEGF) that was serially diluted in a complete culture medium containing 1 nM SLT−VEGF.

liposomes, as demonstrated by fluorescence microscopy (data not shown).

(VEGFR-2)-Targeted Liposomal Formulations of Compound I. The purpose of these studies was to establish that liposomal formulations of compound **I** are also effective in targeting cell receptors other than FR. For this purpose, nontargeted liposomal formulations of compound **I** were decorated with a novel single-chain VEGF (scVEGF) that comprises two 3−112-aa-long fragments of human $VEGF_{121}$ fused head-to-tail (*46*) and expressed with a N-terminal 15-aa Cys tag, a novel cysteine-containing peptide tag for site-specific modification of recombinant proteins (*47*). Cys-tagged scVEGF was site-specifically lipidated with DSPE−PEG(2000)−maleimide at the molar lipid/protein ratio 10:1, and the reaction mixture was added to a nontargeted liposomal formulations of compound **I** for a so-called postinsertion of lipidated scVEGF into the liposomal membrane, as described in Experimental Procedures.

After purification on Sepharose CL-4B, the concentration of scVEGF in the liposomal formulations of compound **I** was determined by Western blot analysis, and the functional activities of the VEGF moiety were tested in two different tissue culture assays. In a short-term (10 min) assay, we tested the ability to induce VEGFR-2 tyrosine autophosphorylation in 293/KDR cells (*44*, *47*, *49*), and in a long-term (72−96 h) assay, we tested the ability to protect 293/KDR cells from VEGFR-2 mediated toxicity of the chimeric toxin SLT−VEGF, comprising a catalytic subunit of Shiga-like toxin and $VEGF_{121}$ (*47*, *49*). As shown in Figures 7 and 8, liposomal (VEGFR-2)-targeted formulations of compound **I** effectively activated VEGFR-2 autophosphorylationin 293/KDR in a nanomolar range typical for these cells (*44*) and protected 293/KDR cells from SLT−

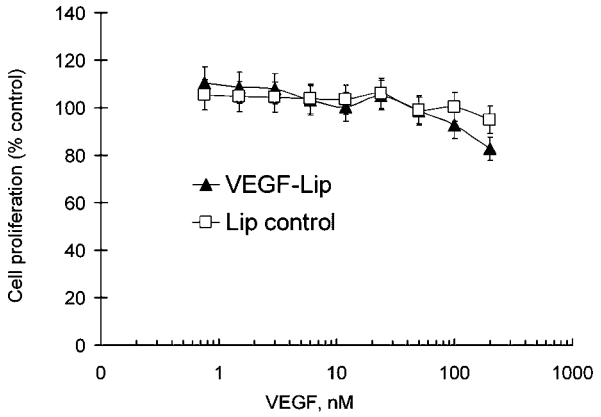

Figure 9. (VEGFR-2)-targeted boronated liposomes are not toxic to VEGFR-2 expressing cells. 293/KDR cells were exposed to indicated amounts of (VEGFR-2)-targeted boronated liposome (VEGF-Lip) or volume equivalents of nontargeted boronated liposomal formulation of compound **I** (Lip control).

VEGF cytotoxicity, although not to the same extent as parental scVEGF. When taken together, these data indicate that boronated (VEGFR-2)-targeted liposomes are indeed effective in targeting VEGFR-2 expressing cells. Furthermore, the data suggest that these liposomes most likely will be internalized via VEGFR-2-mediated endocytosis, as has been demonstrated by us for (VEGFR-2)-targeted liposomes loaded with doxorubicin (*58*).

The cytotoxicity of the (VEGFR-2)-targeted liposomal formulation of compound **I** was evaluated in 293/KDR cells. The cells were plated at low density (1000 cells/well) and allowed to grow for 96 h in the presence of different amounts of either (VEGFR-2)-targeted or nontargeted liposomal formulations of **I**. The obtained results (Figure 9) indicate that neither liposomal formulation affected significantly the growth of 293/KDR cells. Given the recently reported rapid receptor-mediated internalization of VEGF-targeted therapeutic liposomes by 293/KDR cells (*59*), one can expect that these cells also internalize the (VEGFR-2)-targeted liposomal formulations of **I** and that the internalized liposomes are not toxic in the absence of neutron irradiation.

SUMMARY AND CONCLUSIONS

Three carboranyl cholesterol derivatives were synthesized and analyzed applying novel molecular design concepts. All three compounds have structural features and physicochemical properties that are very similar to those of cholesterol. One of the synthesized boronated cholesterol mimics (compound **I**) was stably incorporated into non-, FR-, and (VEGFR-2)-targeted liposomes. No major differences were found in appearance, size distribution, and lamellarity between conventional DPPC/cholesterol liposomes, nontargeted, and FR-targeted liposomal formulations of compound **I**. The calcein release properties of conventional DPPC/cholesterol liposomes and nontargeted boronated liposomes were comparable and were reflected by the boron release rate of the latter. The calcein and boron release rates of FR-targeted boronated liposomes were higher than those of nontargeted boronated liposomes, but the overall stability of the latter was acceptable for the purpose of tumor-selective boron delivery for BNCT. There was no apparent in vitro cytotoxicity to FR overexpressing KB cells and VEGF overexpressing 293/KDR cells when these were incubated with boronated FR- and (VEGFR-2)-targeted liposomal formulations, respectively, although the former accumulated extensively in KB cells, and the latter effectively interacted with VEGFR-2 by causing autophosphorylation and protecting 293/KDR cells from SLT−VEGF cytotoxicity. These results convincingly demonstrate that the novel carboranyl cholesterol mimics are excellent lipid bilayer components for the construction of nontargeted and receptor-targeted boronated liposomes for BNCT of cancer.

ACKNOWLEDGMENT

This work was supported by the U.S. Department of Energy grant DE-FG-2-02ER83520 (J.M.B.) and, in part, by the National Institutes of Health grant R01 CA098945 (R.F.B.). The authors thank Ms. Michele Swindall for technical assistance.

LITERATURE CITED

(1) Barth, R. F., Coderre, J. A., Vicente, M. G. H., and Blue, T. E. (2005) Boron neutron capture therapy of cancer: Current status and future prospects. *Clin. Cancer Res. 11*, 3987−4002.

(2) Shelly, K., Feakes, D. A., Hawthorne, M. F., Schmidt, P. G., Krisch, T. A., and Bauer, W. F. (1992) Model studies directed toward the boron neutron-capture therapy of cancer: boron delivery to murine tumors with liposomes. *Proc. Natl. Acad. Sci. U.S.A. 89*, 9039−9043.

(3) Yanagie, H., Fujii, Y., Tomita, T., Nariuchi, H., Sekiguchi, M., and Kobayashi, H. (1992) Application of boronated anti-CEA immunoliposome to boron neutron capture therapy. In *Progress in Neutron Capture Therapy for Cancer* (Allen, B. J., Moore, D. E., and Harrington, B. V., Eds.) pp 273−275, Plenum Press, New York.

(4) Hawthorne, M. F., and Shelly, K. (1997) Liposomes as drug delivery vehicles for boron agents. *J. Neurooncol. 33*, 53−58.

(5) Yanagie, H., Maruyama, K., Takizawa, T., Ishida, O., Ogura, K., Matsumoto, T., Sakurai, Y., Kobayashi, T., Shinohara, A., Rant, J., Skvarc, J., Ilic, R., Kuhne, G., Chiba, M., Furuya, Y., Sugiyama, H., Hisa, T., Ono, K., Kobayashi, H., and Eriguchi, M. (2006) Application of boron-entrapped stealth liposomes to inhibition of growth of tumour cells in the in vivo boron neutron-capture therapy model. *Biomed. Pharmacother. 60*, 43−50.

(6) Maruyama, K. (2005) Intracellular targeting by transferrin-PEG pendant type liposomes, for boron neutron-capture therapy (BNCT). *Drug Delivery Syst. 20*, 35−41.

(7) Kullberg, E., Wei, Q., Capala, J., Giusti, V., Malmstroem, P.-U., and Gedda, L. (2005) EGF-receptor targeted liposomes with boronated acridine: Growth inhibition of cultured glioma cells after neutron irradiation. *Int. J. Radiat. Biol. 81*, 621−629.

(8) Wei, Q., Kullberg, E. B., and Gedda, L. (2003) Trastuzumab-conjugated boron-containing liposomes for tumor-cell targeting; development and cellular studies. *Int. J. Oncol. 23*, 1159−1165.

(9) Krijger, G. C., Fretz, M. M., Woroniecka, U. D., Steinebach, O. M., Jiskoot, W., Storm, G., and Koning, G. A. (2005) Tumor cell and tumor vasculature targeted liposomes for neutron capture therapy. *Radiochim. Acta 93*, 589−593.

(10) Sudimack, J. J., Adams, D., Rotaru, J., Shukla, S., Yan, J., Sekido, M., Barth, R. F., Tjarks, W., and Lee, R. J. (2002) Folate receptor-mediated liposomal delivery of a lipophilic boron agent to tumor cells in vitro for neutron capture therapy. *Pharm. Res. 19*, 1502−1508.

(11) Pan, X. Q., Wang, H., Shukla, S., Sekido, M., Adams, D. M., Tjarks, W., Barth, R. F., and Lee, R. J. (2002) Boron-containing folate receptor-targeted liposomes as potential delivery agents for neutron capture therapy. *Bioconjugate Chem. 13*, 435−442.

(12) Awad, D., Tabod, I., Lutz, S., Wessolowski, H., and Gabel, D. (2005) Interaction of $Na_2B_{12}H_{11}SH$ with liposomes: Influence on zeta potential and particle size. *J. Organomet. Chem. 690*, 2732−2735.

(13) Mehta, S. C., Lai, J. C. K., and Lu, D. R. (1996) Liposomal formulations containing sodium mercaptoundecahydrododecaborate (BSH) for boron neutron capture therapy. *J. Microencapsulation 13*, 269−279.

(14) Martini, S., Ristori, S., Pucci, A., Bonechi, C., Becciolini, A., Martini, G., and Rossi, C. (2004) Boronphenylalanine insertion in cationic liposomes for boron neutron capture therapy. *Biophys. Chem. 111*, 27−34.

(15) Feakes, D. A., Shelly, K., Knobler, C. B., and Hawthorne, M. F. (1994) $Na_3[B_{20}H_{17}NH_3]$: Synthesis and liposomal delivery to murine tumors. *Proc. Natl. Acad. Sci. U.S.A. 91*, 3029−3033.

(16) Zhou, R., Balasubramanian, S. V., Kahl, S. B., and Straubinger, R. M. (1999) Biopharmaceutics of boronated radiosensitizers: Liposomal formulation of MnBOPP (manganese chelate of 2,4-(α,β-dihydroxyethyl) deuterioporphyrin IX) and comparative toxicity in mice. *J. Pharm. Sci. 88*, 912−917.
(17) Ristori, S., Oberdisse, J., Grillo, I., Donati, A., and Spalla, O. (2005) Structural characterization of cationic liposomes loaded with sugar-based carboranes. *Biophys. J. 88*, 535−547.
(18) Rossi, S., Schinazi, R. F., and Martini, G. (2005) ESR as a valuable tool for the investigation of the dynamics of EPC and EPC/cholesterol liposomes containing a carboranyl-nucleoside intended for BNCT. *Biochim. Biophys. Acta 1712*, 81−91.
(19) Li, T., Hamdi, J., and Hawthorne, M. F. (2006) Unilamellar liposomes with enhanced boron content. *Bioconjugate Chem. 17*, 15−20.
(20) Nakamura, H., Miyajima, Y., Takei, T., Kasaoka, S., and Maruyama, K. (2004) Synthesis and vesicle formation of a *nido*-carborane cluster lipid for boron neutron capture therapy. *Chem. Commun. (Cambridge, U.K.)* 1910−1911.
(21) Feakes, D. A., Shelly, K., and Hawthorne, M. F. (1995) Selective boron delivery to murine tumors by lipophilic species incorporated in the membranes of unilamellar liposomes. *Proc. Natl. Acad. Sci. U.S.A. 92*, 1367−1370.
(22) Firestone, R. A. (1994) Low-density lipoprotein as a vehicle for targeting antitumor compounds to cancer cells. *Bioconjugate Chem. 5*, 105−113.
(23) Ji, B., Peacock, G., and Lu, D. R. (2002) Synthesis of cholesterol-carborane conjugate for targeted drug delivery. *Bioorg. Med. Chem. Lett. 12*, 2455−2458.
(24) Pan, G., Oie, S., and Lu, D. R. (2005) Uptake of the carborane derivative of cholesteryl ester by glioma cancer cells is mediated through LDL receptors. *Pharm. Res. 21*, 1257−1262.
(25) Peacock, G., Sidwell, R., Pan, G., Oie, S., and Lu, D. R. (2004) In vitro uptake of a new cholesteryl carborane ester compound by human glioma cell lines. *J. Pharm. Sci. 93*, 13−19.
(26) Alanazi, F., Halpern, D. S., and Lu, D. R. (2004) Intracerebral diffusion of new cholesterol-based anticancer conjugate in tumor-bearing rat model. *J. Appl. Res. 4*, 127−134.
(27) Feakes, D. A., Spinler, J. K., and Harris, F. R. (1999) Synthesis of boron-containing cholesterol derivatives for incorporation into unilamellar liposomes and evaluation as potential agents for BNCT. *Tetrahedron 55*, 11177−11186.
(28) Setiawan, Y., Moore, D. E., and Allen, B. J. (1996) Selective uptake of boronated low-density lipoprotein in melanoma xenografts achieved by diet supplementation. *Br. J. Cancer 74*, 1705−1708.
(29) Laster, B. H., Kahl, S. B., Popenoe, E. A., Pate, D. W., and Fairchild, R. G. (1991) Biological efficacy of boronated low-density lipoprotein for boron neutron capture therapy as measured in cell culture. *Cancer Res. 51*, 4588−4593.
(30) Leppala, J., Kallio, M., Nikula, T., Nikkinen, P., Liewendahl, K., Jaaskelainen, J., Savolainen, S., Gylling, H., Hiltunen, J., and Callaway, J. (1995) Accumulation of ^{99m}Tc-low-density lipoprotein in human malignant glioma. *Br. J. Cancer 71*, 383−387.
(31) Endo, Y., Iijima, T., Yamakoshi, Y., Fukasawa, H., Miyaura, C., Inada, M., Kubo, A., and Itai, A. (2001) Potent estrogen agonists based on carborane as a hydrophobic skeletal structure: a new medicinal application of boron clusters. *Chem. Biol. 8*, 341−355.
(32) Endo, Y., Iijima, T., Yamakoshi, Y., Yamaguchi, M., Fukasawa, H., and Shudo, K. (1999) Potent estrogenic agonists bearing dicarba-*closo*-dodecaborane as a hydrophobic pharmacophore. *J. Med. Chem. 42*, 1501−1504.
(33) Stephenson, S. M., Low, P. S., and Lee, R. J. (2004) Folate receptor-mediated targeting of liposomal drugs to cancer cells. *Methods Enzymol. 387*, 33−50.
(34) Gosselin, M. A., and Lee, R. J. (2002) Folate receptor-targeted liposomes as vectors for therapeutic agents. *Biotechnol. Annu. Rev. 8*, 103−131.
(35) Cardones, A. R., and Banez, L. L. (2006) VEGF inhibitors in cancer therapy. *Curr. Pharm. Des. 12*, 387−394.
(36) Bergsland, E. K. (2004) Update on clinical trials targeting vascular endothelial growth factor in cancer. *Am. J. Health Syst. Pharm. 61*, S12−S20.
(37) Tai, A., Syouno, E., Tanaka, K., Fujita, M., Sugimura, T., Higashiura, Y., Kakizaki, M., Hara, H., and Naito, T. (2002) Regio- and stereochemical study of sex pheromone of pine sawfly; Diprion nipponica. *Bull. Chem. Soc. Jpn. 75*, 111−121.
(38) Pedretti, A., Villa, L., and Vistoli, G. (2004) VEGA - An open platform to develop chemo-bio-informatics applications, using plug-in architecture and script programming. *J. Comput.-Aided Mol. Des. 18*, 167−173.
(39) Johnsamuel, J., Byun, Y., Jones, T. P., Endo, Y., and Tjarks, W. (2003) A new strategy for molecular modeling and receptor-based design of carborane containing compounds. *J. Organomet. Chem. 680*, 223−231.
(40) Johnsamuel, J., Byun, Y., Jones, T. P., Endo, Y., and Tjarks, W. (2003) A convenient method for the computer-aided molecular design of carborane containing compounds. *Bioorg. Med. Chem. Lett. 13*, 3213−3216.
(41) Fauchere, J. L., Kim Quang, D., Jow, P. Y. C., and Hansch, C. (1980) Unusually strong lipophilicity of 'fat' or 'super' amino acids, including a new reference value for glycine. *Experientia 36*, 1203−1204.
(42) Al-Madhoun, A. S., Johnsamuel, J., Barth, R. F., Tjarks, W., and Eriksson, S. (2004) Evaluation of human thymidine kinase 1 substrates as new candidates for boron neutron capture therapy. *Cancer Res. 64*, 6280−6286.
(43) Guo, W., Lee, T., Sudimack, J., and Lee, R. J. (2000) Receptor-specific delivery of liposomes via folate-PEG-Chol. *J. Liposome Res. 10*, 179−195.
(44) Backer, M. V., and Backer, J. M. (2001) Functionally active VEGF fusion proteins. *Protein Expression Purif. 23*, 1−7.
(45) Lee, R. J., and Low, P. S. (1994) Delivery of liposomes into cultured KB cells via folate receptor-mediated endocytosis. *J. Biol. Chem. 269*, 3198−204.
(46) Backer, M. V., Patel, V., Jehning, B. T., Claffey, K. P., and Backer, J. M. (2006) Surface immobilization of active vascular endothelial growth factor via a cysteine-containing tag. *Biomaterials 27*, 5452−5458.
(47) Backer, M. V., Gaynutdinov, T. I., Patel, V., Bandyopadhyaya, A. K., Thirumamagal, B. T. S., Tjarks, W., Barth, R. F., Claffey, K., and Backer, J. M. (2005) Vascular endothelial growth factor selectively targets boronated dendrimers to tumor vasculature. *Mol. Cancer Ther. 4*, 1423−1429.
(48) Barth, R. F., Adams, D. M., Soloway, A. H., Mechetner, E. B., Alam, F., and Anisuzzaman, A. K. M. (1991) Determination of boron in tissues and cells using direct-current plasma atomic emission spectroscopy. *Anal. Chem. 63*, 890−893.
(49) Backer, M. V., and Backer, J. M. (2001) Targeting endothelial cells overexpressing VEGFR-2: selective toxicity of Shiga-like toxin-VEGF fusion proteins. *Bioconjugate Chem. 12*, 1066−1073.
(50) Goncalves, E., Debs, R. J., and Heath, T. D. (2004) The effect of liposome size on the final lipid/DNA ratio of cationic lipoplexes. *Biophys. J. 86*, 1554−1563.
(51) Lunato, A. J., Wang, J., Woollard, J. E., Anisuzzaman, A. K. M., Ji, W., Rong, F.-G., Ikeda, S., Soloway, A. H., Eriksson, S., Ives, D. H., Blue, T. E., and Tjarks, W. (1999) Synthesis of 5-(carboranylalkylmercapto)-2′-deoxyuridines and 3-(carboranylalkyl)thymidines and their evaluation as substrates for human thymidine kinases 1 and 2. *J. Med. Chem. 42*, 3378−3389.
(52) Fujii, S., Hashimoto, Y., Suzuki, T., Ohta, S., and Endo, Y. (2005) A new class of androgen receptor antagonists bearing carborane in place of a steroidal skeleton. *Bioorg. Med. Chem. Lett. 15*, 227−230.
(53) Eriksson, L., Winberg, K. J., Claro, R. T., and Sjoeberg, S. (2003) Palladium-catalyzed heck reactions of styrene derivatives and 2-iodo-*p*-carborane. *J. Org. Chem. 68*, 3569−3573.
(54) Cohen, N., Scott, C. G., Neukom, C., Lopresti, R. J., Weber, G., and Saucy, G. (1981) Total synthesis of all eight stereoisomers of α-tocopheryl acetate. Determination of their diastereoisomeric and enantiomeric purity by gas chromatography. *Helv. Chim. Acta 64*, 1158−1173.
(55) Gabizon, A., and Papahadjopoulos, D. (1988) Liposome formulations with prolonged circulation time in blood and enhanced uptake by tumors. *Proc. Natl. Acad. Sci. U.S.A. 85*, 6949−6953.
(56) Cirli, O. O., and Hasirci, V. (2004) UV-induced drug release from photoactive REV sensitized by suprofen. *J. Controlled Release 96*, 85−96.
(57) Elwood, P. C., Kane, M. A., Portillo, R. M., and Kolhouse, J. F. (1986) The isolation, characterization, and comparison of the

membrane-associated and soluble folate-binding proteins from human KB cells. *J. Biol. Chem. 261*, 15416−15123.
(58) Backer, M. V., Gaynutdinov, T. I., Patel, V., Myshkin, E., and Backer, J. M. (2004) Adapter protein for site-specific conjugation of payloads for targeted drug delivery. *Bioconjugate Chem. 15*, 1021−1029.
(59) Backer, M. V., Patel, V., Jehning, B. T., and Backer, J. M. (2006) Self-assembled "dock and lock" system for linking payloads to targeting proteins. *Bioconjugate Chem. 4*, 912−919.

BC060075D